

INORGANIC OPTICAL COATINGS FOR PHOTONIC DEVICES WORKING AT VISIBLE FREQUENCY

White paper
2025

Marco Abbarchi^{1,*}, Dominique Bonisseau¹, Mohammed Bouabdellaoui¹, Arthur Clini de Souza^{1,2}, Elie Daher¹, Anthony Gourdin¹, Charlotte Grosso¹, David Grosso¹, Mahmoud Elsayw², Olivier Hector¹, Badre Kerzabi¹, Stephane Lanteri², Lisa Weber¹

¹ SOLNIL, Pépinière d'Entreprises Luminy Biotech, 163 avenue de Luminy, 13011 Marseille, France

² Université Côte d'Azur, INRIA, CNRS, LJAD, 06902 Sophia Antipolis cedex, France

EXECUTIVE SUMMARY

This white paper presents an in-depth overview of optical coatings tailored for photonic devices operating in the visible frequency range (~380 -750 nm). It emphasizes the critical role of material properties, such as refractive index, extinction coefficient, and density, in defining the performance of optical components as well as their deposition processes. The key focus of the document is on the state-of-the-art in inorganic materials, highlighting metal oxides, silicon carbide, fluorides, and nitrides as essential building blocks for advanced photonic devices.

In particular, SOLNIL's innovative liquid chemistry approach is showcased for its ability to produce fully inorganic thin films with exceptional optical properties. This process enables the production of ultra-high refractive index TiO_2 coatings (with n from 1.7 up to 2.60) and ultra-low refractive index SiO_2 films (with n down to 1.12 up to 1.5) using simple, cost-effective deposition techniques, such as spin-coating and dip-coating under ambient conditions. All the intermediate values of refractive index between 1.12 and 2.6 can be obtained by simple mixing two liquid solutions. These films exhibit remarkable uniformity and extremely low scattering losses featuring reduced surface roughness (below 1 nm RMS), making them highly suitable for applications ranging from anti-reflection coatings to photonic integrated circuits and meta-surfaces.

The transformative potential of SOLNIL's technologies in advancing next-generation photonic devices for imaging, sensing, and beyond starts from the materials.

Keywords: Inorganic Materials, Optical Coating, Photonic Device, Visible Frequency, Liquid Chemistry, Thin Film Deposition, TiO_2 , SiO_2 , Ultra-High Refractive Index, Ultra-Low Refractive Index, Meta-surfaces, Bragg Mirrors, Photonic Integrated Circuits, Refractive Index Contrast, Anti-Reflection Coatings

ACKNOWLEDGMENTS



We acknowledge the following projects and funding scheme:

-IC TRANSITION METAPRINT (n.101202776)

PIA4 METANANOGRILLE (DOS0254908/00 et DOS0254909/00)

ANR DNN4PHOTONICS (ANR-24-CE24-3100)

PHOTONHUB EUROPE (n. 101016665)

I-LAB METANIL (DOS0197628/00)

DGA ARES (n.2025 20 0928)

INORGANIC OPTICAL COATINGS FOR PHOTONIC DEVICES WORKING AT VISIBLE FREQUENCY

Marco Abbarchi^{1,*}, Dominique Bonisseau¹, Mohammed Bouabdellaoui¹, Arthur Clini de Souza^{1,2}, Elie Daher¹, Anthony Gourdin¹, Charlotte Grosso¹, David Grosso¹, Mahmoud Elsayy², Olivier Hector¹, Badre Kerzabi¹, Stephane Lanteri², Lisa Weber¹

¹ SOLNIL, Pépinière d'Entreprises Luminy Biotech, 163 avenue de Luminy, 13011 Marseille, France

² Université Côte d'Azur, INRIA, CNRS, LJAD, 06902 Sophia Antipolis cedex, France

*marco.abbarchi@solnil.com

ABSTRACT. Optical components, photonic integrated circuits (PICs), and meta-surfaces working in the visible spectrum are revolutionizing imaging, displays, sensing, and communications by precisely controlling light at sub-wavelength scales. Nano-photonic devices mirror electronic circuits for light, enabling breakthroughs in biomedical imaging, quantum optics, AR displays, wearables, optical interconnects, and lab-on-chip systems. Meta-surfaces, ultra-thin, engineered 2D layers, replace bulky optics with efficient lenses, holographic displays, structural colours, and anti-reflection coatings, ideal for next-gen AR/VR, microscopy, sensors, and point-of-care diagnostics. High-power visible and near-UV lasers are now widely used in precision material processing, high-resolution imaging, and medical procedures, thanks to advancements in fabrication and materials. As techniques improve, we can expect meta-surface lenses to supplant conventional optics in cameras and displays, compact colour filters, diffractive and holographic transparent displays, ultra-sensitive sensors, and mass-produced visible-wavelength PICs, each tailored with application-specific materials and fabrication methods. **With a very broad range of application and highly segmented market landscape, each sector will exploit different materials and fabrication methods (both for thin 2D films and 3D structures) depending on quality, cost and device volumes.**

The range of uses of a material directly depends on its intrinsic features (e.g. crystalline state, refractive index) as well as its processability (e.g. the possibility to deposit it as a high-quality thin film or shape it as a 3D structure). Here, we first introduce the main features of a material that directly impact its optical properties. Then, we provide a non-exhaustive list of materials relevant to applications at visible frequency and the corresponding methods of deposition as thin films. **Finally, we discuss the case of inorganic resin-based materials developed by SOLNIL, specifically ultra-high refractive index TiO₂ (n = 2.6) and ultra-low refractive index SiO₂ (n = 1.12). We show how they are obtained, their features and performances including examples of potential applications.**

SOLNIL stands at the cutting edge of material engineering, revolutionizing thin film coatings with innovative solutions. By harnessing advanced inorganic chemistry and pioneering liquid deposition techniques for metal oxides, SOLNIL delivers materials with ultra-high and ultra-low refractive indices, achieving unparalleled performance. Utilizing straightforward deposition methods like spin- and dip-coating at room temperature and ambient pressure, SOLNIL ensures wafer-level scalability and customizable optical properties. This ground-breaking approach is set to transform advanced materials for visible frequency applications.

TABLE OF CONTENTS

EXECUTIVE SUMMARY.....	1
ACKNOWLEDGMENTS	1
INORGANIC OPTICAL COATINGS FOR PHOTONIC DEVICES WORKING AT VISIBLE FREQUENCY	2
1. OPTICAL PROPERTIES OF INORGANIC MATERIALS FOR APPLICATIONS AT VISIBLE FREQUENCY	4
1.1. ORGANIC VS INORGANIC MATERIALS	4
1.2 REFRACTIVE INDEX AND EXTINCTION COEFFICIENT	4
1.3. REFRACTIVE INDEX AND MATERIAL DENSITY	5
2. MATERIALS FOR OPTICS AND PHOTONICS AT VISIBLE FREQUENCY.....	6
3. THIN FILM DEPOSITION METHODS	10
4. SOLNIL’S WAY: INORGANIC RESIST SOLUTIONS FOR OPTICAL THIN FILMS MADE OF FULLY INORGANIC MATERIALS	12
4.1. SOLNIL’S ULTRA-HIGH AND ULTRA-LOW REFRACTIVE INDEX MATERIALS	13
4.2. SOLNIL: TWO SOLUTIONS FOR ALL THE REFRACTIVE INDICES	15
4.3. IMPACT OF THE REFRACTIVE INDEX CONTRAST	17
4.3.1. LIGHT GUIDING	17
4.3.2. BRAGG STRUCTURES	18
4.4.3. PHOTONIC META-SURFACES.....	19
5. CONCLUSION	20

1. OPTICAL PROPERTIES OF INORGANIC MATERIALS FOR APPLICATIONS AT VISIBLE FREQUENCY

1.1. ORGANIC VS INORGANIC MATERIALS

A first discrimination between **materials for optics and photonics working at visible frequency** is between organic and inorganic ones. **Organic materials** typically refer to substances like polymers, and organic dyes^{1,2,3}. They are generally characterized by their ease of processing, often via solution processing, and can be engineered to have tuneable optical properties through chemical modifications, doping, and nano-structuring. In the visible frequency range, organic materials can exhibit high luminescence efficiency and offer flexibility in design, which makes them attractive for applications such as flexible displays, light-emitting devices, optical sensors, and structural colours. **However, they often have relatively small refractive index and high optical loss due to scattering, absorption and inhomogeneity. At the same time they face limitations in terms of thermal and photochemical stability; prolonged exposure to humidity, UV radiation, intense visible light or elevated temperatures can lead to degradation (yellowing, loss of transparency, or reduced emission efficiency). In short, they are susceptible to photobleaching, oxidation, thermal degradation leading to relatively short lifetime.**

In contrast, **inorganic materials**-such as glasses, crystalline or amorphous semiconductors/insulators, and ceramics, tend to have superior optical clarity, thermal stability, and durability^{4,5,6,7}. Their high refractive indices and low absorption and scattering losses across broad spectral ranges make them ideal for high-performance lenses, mirrors, and waveguides used in imaging and telecommunications. Although they usually require more energy-intensive processing methods (e.g., high-temperature annealing, chemical vapour deposition, or precision machining), the resulting components are robust and reliable over long operational lifetimes.

Thus, the main difference lies in their trade-offs: organic materials offer design flexibility and simpler, lower-cost processing at the expense of stability and longevity, while inorganic materials deliver excellent optical performance and durability, albeit with more complex and higher-cost fabrication techniques.

Here we focus on inorganic materials for top-end applications, where durability and performances are necessary requirements.

1.2 REFRACTIVE INDEX AND EXTINCTION COEFFICIENT

The **refractive index (n)** is a fundamental optical property of a material that measures how much light slows down when passing through it^{8,9,10}. It relates to the phase velocity ($n = c/v_p = \lambda/\lambda_0$, where c is the speed of light in vacuum, v_p is the speed of light in the material and λ (λ_0) is the wavelength of light in the material (vacuum)). A **higher refractive index** means light has a shorter wavelength, travels more slowly through the material and bends more at interfaces (Snell's Law)⁸. This property is crucial in designing lenses, thin films, optical fibers, and meta-surfaces, as it determines how efficiently light can be controlled. For example, air has a refractive index of **~1.0**, while glass is around **1.5**, whereas titanium dioxide (TiO₂) and silicon carbide (SiC) can reach **~2.6**, making them excellent materials for strong optical confinement.

The optical loss are described by the **extinction coefficient (k)** measuring how much light is absorbed or scattered as it propagates through a material^{11,12}. It is part of the **complex refractive index $\tilde{n} = n - ik$** . A **higher k** means stronger absorption/scattering, while a **low k** is the signature for transparent materials. Thus **k** enters in the Beer-Bouguer-Lambert extinction law (e.g. for a plane wave of intensity $I(x)$ propagating along the x direction) via:

¹ O'Neill, Mary, and Stephen M. Kelly. "Ordered materials for organic electronics and photonics." *Advanced Materials* 23.5 (2011): 566-584.

² Clark, Jenny, and Guglielmo Lanzani. "Organic photonics for communications." *Nature photonics* 4.7 (2010): 438-446.

³ Frka-Petesic, Bruno, et al. "Structural color from cellulose nanocrystals or chitin nanocrystals: self-assembly, optics, and applications." *Chemical Reviews* 123.23 (2023): 12595-12756.

⁴ Choudhary, Ram Naresh Prasad, and Sunanda Kumari Patri. *Dielectric materials: introduction, research and applications*. xx: Nova Science Publishers, 2009.

⁵ Fiedziuszko, S. Jerry, et al. "Dielectric materials, devices, and circuits." *IEEE Transactions on microwave theory and techniques* 50.3 (2002): 706-720.

⁶ Krasnok, Alexander, et al. "Towards all-dielectric metamaterials and nanophotonics." *Metamaterials X*. Vol. 9502. SPIE, 2015.

⁷ Baranov, Denis G., et al. "All-dielectric nanophotonics: the quest for better materials and fabrication techniques." *Optica* 4.7 (2017): 814-825.

⁸ Born, Max, and Emil Wolf. *Principles of optics: electromagnetic theory of propagation, interference and diffraction of light*. Elsevier, 2013.

⁹ Singh, Shyam. "Refractive index measurement and its applications." *Physica Scripta* 65.2 (2002): 167.

¹⁰ Heller, Wilfried. "Remarks on refractive index mixture rules." *The Journal of Physical Chemistry* 69.4 (1965): 1123-1129.

¹¹ Polyanskiy, Mikhail N. "Refractiveindex. info database of optical constants." *Scientific Data* 11.1 (2024): 94.

¹² Zhao, J., and J. M. Cole. "A database of refractive indices and dielectric constants auto-generated using chemdataextractor. *Scientific Data* 9." 2022

$$I(x) = I_0(x)e^{-4\pi kx/\lambda_0}$$

In presence of an extinction coefficient, light undergoes an exponential decay while propagating in a medium and the penetration depth (the distance δ_p after which the intensity is reduced by a factor of $1/e$) is $\delta_p = 1/\alpha_{abs} = \lambda_0/4\pi k$. Real (n) and imaginary (k) parts of \tilde{n} are linked by the Kramers-Kronig relations¹³ and they always depend on the frequency of the light, leading to the light dispersion.

Losses arise from two main mechanisms: **absorption** (light energy is converted into heat or electronic excitations), and **scattering** (light is redirected due to imperfections, grain boundaries, or nano-scale roughness). While scattering does not directly increase k , it reduces the transmitted light, leading to effective optical losses. k primarily accounts for absorption losses, whereas high scattering can make effective k appear larger in experimental measurements if light is redirected rather than transmitted. This is particularly relevant in **nano-structured and rough materials**, where distinguishing between absorption and scattering losses is challenging.

Transparent materials (e.g. SiO_2 , TiO_2) have almost near-zero k in the visible range and quite small dispersion, making them ideal for lenses, waveguides, and meta-surfaces. **Low-loss dielectrics** with small k are crucial for high-efficiency photonic devices, as they minimize energy dissipation and unwanted heating. Balancing n and k is key in designing **high-performance optical systems**, from anti-reflection coatings to high-efficiency meta-surfaces. Let's also mention that **absorbing materials** with high k (e.g., metals) have important applications for plasmonics and thermal emission control.

1.3. REFRACTIVE INDEX AND MATERIAL DENSITY

The **refractive index n** of a material is strongly influenced by its **density** and thus by its **crystalline structure**. In general, a higher density and a well-ordered crystalline state lead to a higher refractive index due to increased electronic polarizability: n is related to the material's density ρ through the **Clausius Mossotti formula**¹⁴:

$$\frac{n^2 - 1}{n^2 + 2} = A \frac{\rho}{M}$$

where A is a proportionality term related to the material's electronic polarizability (generally dependent on frequency), and M is the molar mass.

The density ρ of a material is influenced by its atomic arrangement, packing efficiency, and the presence of micro- and meso-porosity. The atomic-scale structure, **crystalline, polycrystalline, or amorphous**, determines the intrinsic density, while porosity at different scales affects the effective density. As a general guideline, materials with higher density usually exhibit higher refractive indices due to tightly bound atoms that enhance electronic polarization (e.g. crystalline solids); **porous or low-density materials** (e.g., sol-gel oxides, aerogels) have lower refractive indices due to reduced polarizability.

Porosity can be introduced at different scales, further reducing the **effective density** and altering the material's optical and mechanical properties:

-Micro-porosity (< 2 nm pores) occurs at the atomic or nano-scale due to defects, grain boundaries, or material processing. It reduces density slightly but can still impact light scattering and optical losses.

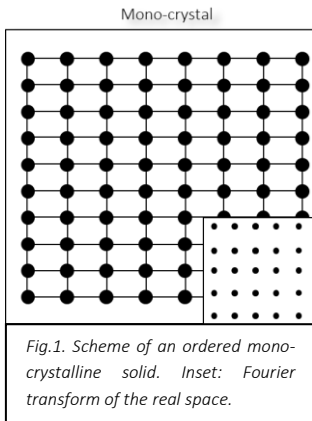
-Meso-porosity (2-50 nm pores) significantly decreases density and can lead to strong light diffusion. Controlled mesoporous structures are used to tune refractive index.

-Macro-porosity (> 50 nm pores) originates from an interconnected network of large voids making these materials ideal for applications such as filtration, catalysis, and tissue engineering. These large pores enable the diffusion of macromolecules and even cells. These materials allow for novel optical effects such as enhanced light scattering, controlled refractive index gradients.

¹³ Lucarini, Valerio, et al. *Kramers-Kronig relations in optical materials research*. Berlin, Heidelberg: Springer Berlin Heidelberg, 2005.

¹⁴ Talebian, E., and M. Talebian. "A general review on the derivation of Clausius-Mossotti relation." *Optik* 124.16 (2013): 2324-2326.

Monocrystalline Solids (Fig.1). Mono-crystals have a perfectly ordered atomic structure with no grain boundaries, leading to highly uniform electronic and optical properties. Their dielectric constant is well-defined and anisotropic in many cases, meaning it varies with direction due to the ordered arrangement of atoms. This is particularly important in *birefringent materials*, where different crystallographic axes exhibit different refractive indices. The absence of grain boundaries reduces scattering losses, enhancing optical transparency and minimizing dielectric losses in applications like high-performance optics.

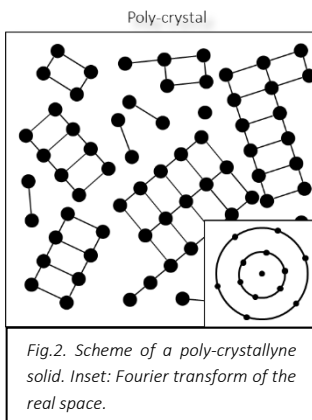


Density: Close to the theoretical maximum for the material.

Effect of Porosity: Generally negligible unless artificially introduced via defects or controlled doping.

Impact on Optical Properties: Low scattering losses, and well-defined refractive index.

Polycrystalline Solids (Fig.2). Poly-crystals consist of multiple small crystalline grains with different orientations, separated by grain boundaries. The dielectric constant is usually an average of the properties of individual grains. However, grain boundaries introduce additional effects, such as charge trapping, increased scattering, and localized variations in polarization. This can lead to slightly lower dielectric constants and higher losses compared to mono-crystals, especially at high frequencies. Polycrystalline materials are often easier and cheaper to produce, making them widely used in commercial optics and electronic devices.

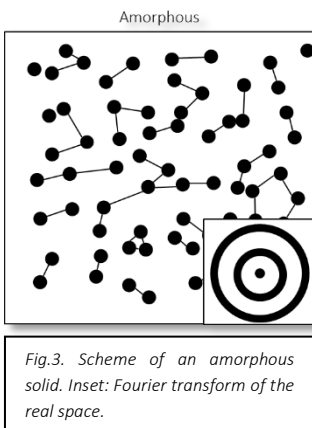


Density: Lower than mono-crystalline but still relatively high.

Effect of Porosity: Grain boundaries may introduce micro-voids, but the overall porosity is still low, unless additional porosity is intentionally introduced.

Impact on Optical Properties: Higher scattering compared to mono-crystals, leading to optical losses at shorter wavelength.

Amorphous Solids (Fig.3). Amorphous materials lack long-range atomic order, meaning their dielectric properties are more isotropic but generally lower than their crystalline counterparts. The lack of a periodic structure results in increased electronic disorder, which can lead to higher optical absorption and reduced dielectric constant. However, the absence of grain boundaries can sometimes reduce charge trapping effects seen in poly-crystals. Amorphous materials like silicon dioxide (SiO_2) are widely used in optical coatings and insulating layers in electronics due to their stability and uniformity.



Density: Lower than both dense mono-crystalline and polycrystalline forms.

Effect of Porosity: Often more susceptible to natural voids or free volume, further decreasing density.

Impact on Optical Properties: lack of scattering thanks to high uniformity at the price of a lower refractive index.

2. MATERIALS FOR OPTICS AND PHOTONICS AT VISIBLE FREQUENCY

Overall, the selection of optical materials for visible photonics depends on the balance between refractive index, optical transparency, abundance, processability, and compatibility with existing fabrication methods. High-index dielectrics excel in photonic devices requiring strong light confinement (e.g. guided optics, resonators, meta-surfaces), low-index materials are indispensable for coatings and protective layers, and polymeric composites expand the possibilities for flexible and lightweight optical systems.

We identify four main categories of inorganic materials: **metal oxides, silicon carbide, fluorides, and nitrides**. Together, they represent a crucial class of materials for visible photonics, offering a combination of high refractive indices, optical transparency, and compatibility with advanced fabrication techniques.

MOx

Metal oxides (MOx), are a broad category of materials composed of metal cations bonded to oxygen anions¹⁵. They can form crystalline and amorphous structures and exhibit a wide range of electrical, optical, and mechanical properties depending on the metal species and oxidation state. In photonics and optics, metal oxides are primarily valued for their **dielectric properties, wide bandgaps, and high transparency in the visible spectrum (400-750 nm)**. They can be engineered to provide refractive indices ranging from low (e.g. silica SiO₂) to high (e.g. titania TiO₂ and niobia Nb₂O₅) and can be processed using various deposition methods, including sol-gel processing, atomic layer deposition (ALD), and sputtering. Their ability to form dense, smooth, and stable thin films makes them ideal for antireflection coatings, optical filters, and high-contrast photonic structures.

SiC

Silicon carbide (SiC) is a **wide-bandgap semiconductor** composed of silicon (Si) and carbon (C) atoms arranged in a covalently bonded crystal structure^{16, 17}. It exists in multiple polytypes, with **4H-SiC and 6H-SiC** being the most common for electronic and photonic applications. SiC thin films can be deposited using **chemical vapour deposition (CVD), physical vapour deposition (PVD), and ion beam sputtering**, providing high-quality, smooth coatings for optical applications. **4H-SiC and 6H-SiC** exhibit significant birefringence due to their hexagonal crystal structures; **3C-SiC** (cubic SiC) shows lower birefringence because of its cubic symmetry. Due to its **high refractive index (~2.6 at 600 nm), excellent transparency in the visible and near-infrared range, and exceptional thermal and mechanical stability**, SiC is used in photonics, power electronics. In photonics, SiC is particularly valuable for **nonlinear optics, quantum photonics¹⁸, and integrated photonic circuits** due to its strong $\chi^{(2)}$ and $\chi^{(3)}$ **nonlinear optical coefficients**, making it suitable for frequency conversion and optical modulation. It also exhibits high **thermal conductivity**, allowing for efficient heat dissipation in high-power optical and electronic devices. Its robustness, wide bandgap (~2.3-3.3 eV), and low optical loss make it an emerging material for **micro-resonators, quantum optics and bio-sensing applications**.

MFx

Fluorides (compounds that incorporate fluorine), examples of which include magnesium fluoride (MgF₂), calcium fluoride (CaF₂), lithium fluoride (LiF), and lanthanum fluoride (LaF₃), are prized in optics for their **excellent transparency across a wide spectral range (especially in the deep-UV and infrared), low refractive index, and low dispersion^{19, 20}**. These properties make them ideal for anti-reflective coatings, lenses, prisms, and windows in high-performance optical systems. Bulk fluoride crystals are typically produced using controlled crystal growth methods such as the Czochralski or Bridgman techniques, which allow for high purity and structural perfection. **For thin-film applications, physical vapour deposition methods, including thermal evaporation and sputtering, are commonly employed to deposit uniform layers of fluoride materials onto various substrates**. These approaches, by ensuring minimal optical losses and high durability, underpin the widespread use of fluoride materials in advanced photonic devices.

SiN GaN

Nitrides (compounds composed of nitrogen and one or more metallic or semiconducting elements) exhibit strong **covalent bonding**, resulting in high mechanical hardness and durability^{21, 22}. They can be deposited using various methods such as **chemical vapour deposition, plasma-enhanced CVD, molecular beam epitaxy, and sputtering**, allowing for precise thickness control and smooth surface morphology. In photonics and optics, nitrides are particularly valued for their **high refractive index, wide bandgap, and excellent thermal and chemical stability**. They are commonly used in

¹⁵ Yu, Xinge, Tobin J. Marks, and Antonio Facchetti. "Metal oxides for optoelectronic applications." *Nature materials* 15.4 (2016): 383-396.

¹⁶ Yi, Ailun, et al. "Silicon carbide for integrated photonics." *Applied Physics Reviews* 9.3 (2022).

¹⁷ Ou, Haiyan, et al. "Novel photonic applications of silicon carbide." *Materials* 16.3 (2023): 1014.

¹⁸ Lohrmann, Alexander, et al. "A review on single photon sources in silicon carbide." *Reports on Progress in Physics* 80.3 (2017): 034502.

¹⁹ Nazabal, Virginie, et al. "Fluoride and oxyfluoride glasses for optical applications." *Journal of Fluorine Chemistry* 134 (2012): 18.

²⁰ Zhu, Xiushan, and N. Peyghambarian. "High-power ZBLAN glass fiber lasers: Review and prospect." *Advances in Optoelectronics* 2010.1 (2010): 501956.

²¹ Moustakas, Theodore D., and Roberto Paiella. "Optoelectronic device physics and technology of nitride semiconductors from the UV to the terahertz." *Reports on Progress in Physics* 80.10 (2017): 106501.

²² Xie, Rong-Jun, and Hubertus T. Hintzen. "Optical properties of (oxy) nitride materials: a review." *Journal of the American Ceramic Society* 96.3 (2013): 665-687.

integrated photonics, optical coatings, and high-power optoelectronic devices. In optics, silicon nitride (Si_3N_4) is one of the most widely used materials due to its moderate-to-medium refractive index (~ 2.0 at 600 nm), low optical losses in the visible and near-infrared range, and compatibility with CMOS fabrication techniques. It is commonly employed in photonic integrated circuits, waveguides, and high-Q resonators. Other nitrides, such as gallium nitride (GaN), are essential in optoelectronics, particularly for light emitting diodes and laser diodes operating in the blue and UV ranges.

A more extensive (but not exhaustive) list of materials and their features is provided in **Table 1 Optical Materials for Visible Photonics (400-750 nm)**. This table serves as a reference for selecting materials based on their optical properties, manufacturability, and performance in applications like coatings, waveguides, and meta-surfaces. The materials are split in three main categories based on their refractive index n :

-**High-refractive index: $n > 2.3$** . Used in high-contrast photonic waveguides, meta-surfaces, resonators, high-efficiency lenses, and light-trapping structures.

-**Medium-refractive index: $(1.6 < n < 2.3)$** . Ideal for dielectric mirrors, anti-reflection coatings, gradient-index optics, and optical filters. Common materials include silicon nitride and certain sol-gel oxides

-**Low-refractive index: $(n < 1.6)$** . Essential for cladding layers in optical waveguides, protective coatings, and broadband anti-reflection coatings.

In Table 1 we consider only materials having an extinction coefficient sufficiently low to be neglected at visible frequency. We do not include the scattering losses (that might come from surface roughness, porosity and grains), that typically depend on the fabrication method for material deposition. For each material is reported:

1) the refractive index n at visible frequency (red, green and blue channels, R, G, and B, respectively), referring to the highest value that can be reached for dense materials usable for applications in photonics (e.g. that do not scatter light). Most values of n for the materials mentioned in Table 1 can be found through this reference²³;

2) the different crystal phases;

3) the main fabrication methods: Sol-gel; Atomic Layer Deposition, ALD; Sputtering; Chemical Vapour deposition, CVD; Metal Organic Chemical Vapour deposition, MOCVD; Liquid Phase Chemical Vapour deposition, LPCVD; Physical Vapour Deposition, PVD; Hydride Vapour Phase Epitaxy, HVPE; solution processing; Thermal Oxidation; Pulsed Laser Deposition, PLD;

4) the main features of the materials, availability, costs, and main uses;

5) advantages and disadvantages (Pros/Cons).

TABLE 1. Table: Optical Materials for Visible Photonics (400-750 nm)					
Material	n (R, G, B)	Crystal Structure /Amorphous	Fabrication Methods	Features/Availability/Cost: Low L, Medium M, High H	Pros/Cons
HIGH REFRACTIVE INDEX					
Titanium Dioxide ^{24,25,26} TiO_2	2.4, 2.5, 2.7 ²⁷	Anatase, Rutile, Brookite, Amorphous	Sol-gel, spray, ALD, Sputter., PECVD, MOCVD	Scalable/Widely available/L-M	High RI, used in coatings, meta-surfaces/Brittle, difficult to pattern at nano-scale
Silicon Carbide ^{16,17,18} SiC	2.55, 2.6, 2.65 ²⁸	Hexagonal, Cubic, Rhombohedral	CVD	High durability, wide band-gap/Limited/H	High thermal and mechanical stability/Expensive, difficult to etch
Niobium Pentoxide ²⁹ , Nb_2O_5	2.2, 2.3, 2.4 ³⁰	Orthorhombic, Amorphous	Sputter., Sol-gel, spray, ALD, PECVD, MOCVD	Dielectric, low optical loss/ Available/M	High RI, good transparency/More expensive than TiO_2 , requires precise processing

²³ <https://refractiveindex.info/?shelf=main&book=Ag&page=Johnson>

²⁴ Diebold, Ulrike. "The surface science of titanium dioxide." *Surface science reports* 48.5-8 (2003): 53-229.

²⁵ Haider, Adawiyah J., Zainab N. Jameel, and Imad HM Al-Hussaini. "Review on: titanium dioxide applications." *Energy Procedia* 157 (2019): 17-29.

²⁶ <https://refractiveindex.info/?shelf=main&book=TiO2&page=Devore-o>

²⁷ <https://refractiveindex.info/?shelf=main&book=TiO2&page=Devore-o>

²⁸ <https://refractiveindex.info/?shelf=main&book=SiC&page=Singh-o>

²⁹ Rani, Rozina Abdul, et al. "Thin films and nanostructures of niobium pentoxide: fundamental properties, synthesis methods and applications." *Journal of Materials Chemistry A* 2.38 (2014): 15683-15703.

³⁰ <https://refractiveindex.info/?shelf=main&book=Nb2O5&page=Franta>

Gallium Nitride ^{31,32} GaN	2.3, 2.4, 2.5 ³³	Wurtzite	MBE, PECVD, MOCVD, ALD, PLD, HVPE	Strong nonlinear properties, blue LEDs & lasers/Commercially available/ H	Good for blue and UV light emission/ Processing complexity
MEDIUM REFRACTIVE INDEX					
TiO ₂ -loaded Polymers ^{34,35}	1.7-2.3	Amorphous (Polymeric Matrix)	Spin-coating	Flexible, printable, tunable RI/Emerging/ L-M	Processable via soft lithography, lightweight/ Hybrid organic/inorganic; Lower RI than TiO₂
Zirconium Dioxide ^{36,37,38} , ZrO ₂	2.0, 2.1, 2.2 ³⁹	Monoclinic, Tetragonal, Cubic, Amorphous	Sol-gel, ALD, PVD, CVD	High optical stability/Widely available/ M	High mechanical and thermal stability/ Lower RI than TiO₂
Zinc-Oxide ^{40,41} , ZnO ₂	2.0, 2.1, 2.2 ⁴²	Hexagonal Wurtzite, amorphous	Sol-gel, PVD, PLD, Sol-gel, CVD, ALD, Hydrothermal	Wide band-gap, piezoelectric, conductive/Readily Available/ L	Abundant, inexpensive, low temperature growth/ difficult p-doping, sensitive to environment
Tantalum Pentoxide ^{43,44} , Ta ₂ O ₅	2.1, 2.15, 2.2 ⁴⁵	Orthorhombic, Amorphous	Sol-gel, PVD, ALD, CVD	Low loss, good for waveguides/Available/ M-H	High RI, low optical loss/ More expensive than TiO₂ and ZrO₂
Hafnium oxide ^{46,47} , HfO ₂	2.1, 2.2, 2.3 ⁴⁸	Monoclinic	Sol-gel, ALD, CVD, sputter.	Wide band-gap used for thin films/Widely available/ M-H	Superior dielectric properties, C-MOS compatible/ Difficult processing
Aluminum Oxide ^{49,50} , Al ₂ O ₃ , Sapphire	1.7, 1.71, 1.72 ⁵¹	Corundum (Hexagonal), Amorphous	Sol-gel, ALD, Sputter., CVD	High durability, good optical quality/Available/ M-H	Mechanically robust, high thermal stability/ Expensive processing
Silicon Nitride ^{52,53} , Si ₃ N ₄	1.98, 2.00, 2.05 ⁵⁴	β-Si ₃ N ₄ Hexagonal), Amorphous	LPCVD, PECVD, Sputter.	Low optical loss/Widely available/ L-M	CMOS-compatible, high durability, used in photonic circuits/ Harder to etch than SiO₂
LOW REFRACTIVE INDEX					
Silicon Dioxide ^{55,56}	1.45, 1.46, 1.47 ⁵⁷	Trigonal, Amorphous:	Sol-gel, Thermal oxidation, PECVD,	High transparency, high thermal stability/Widely	Used in optical fibers, coatings/ Low refractive index

³¹ Amir, Husam Aldin A. Abdul, Makram A. Fakhri, and Ali Abdulkhaleq Alwahib. "Review of GaN optical device characteristics, applications, and optical analysis technology." *Materials Today: Proceedings* 42 (2021): 2815-2821.

³² Bakar, Mohamad Aizat Abu, et al. "GaN film optical nonlinearity: wavelength dependent refractive index for All-Optical switching application." *Optics & Laser Technology* 166 (2023): 109642.

³³ <https://refractiveindex.info/?shelf=main&book=GaN&page=Barker-o>

³⁴ Chaudhari, Satyaieet, Tasnim Shaikh, and Priyesh Pandey. "A review on polymer TiO₂ nanocomposites." *Int J Eng Res Appl* 3.5 (2013): 1386-1391.

³⁵ Tekin, Derya, Derya Birhan, and Hakan Kiziltaş. "Thermal, photocatalytic, and antibacterial properties of calcinated nano-TiO₂/polymer composites." *Materials Chemistry and Physics* 251 (2020): 123067.

³⁶ Horti, N. C., et al. "Structural and optical properties of zirconium oxide (ZrO₂) nanoparticles: effect of calcination temperature." *Nano Express* 1.1 (2020): 010022.

³⁷ Bocanegra-Bernal, M. H., and S. Díaz De La Torre. "Phase transitions in zirconium dioxide and related materials for high performance engineering ceramics." *Journal of materials science* 37.23 (2002): 4947-4971.

³⁸ Fedorov, Pavel P., and Evgeniya G. Yarotskaya. "Zirconium dioxide. Review." *Конденсированные среды и межфазные границы* 23.2 (eng) (2021): 170-188.

³⁹ <https://refractiveindex.info/?shelf=main&book=ZrO2&page=Wood>

⁴⁰ Klingshirn, Claus F., et al. "Zinc oxide: from fundamental properties towards novel applications." (2010).

⁴¹ Vyas, Sumit. "A short review on properties and applications of zinc oxide based thin films and devices: ZnO as a promising material for applications in electronics, optoelectronics, biomedical and sensors." *Johnson matthey technology review* 64.2 (2020): 202-218.

⁴² <https://refractiveindex.info/?shelf=main&book=ZnO&page=Bond-o>

⁴³ Zhang, Cheng, et al. "Tantalum pentoxide: a new material platform for high-performance dielectric metasurface optics in the ultraviolet and visible region." *Light: Science & Applications* 13.1 (2024): 23.

⁴⁴ Ezhilvalavan, S., and Tseung-Yuen Tseng. "Preparation and properties of tantalum pentoxide (Ta₂O₅) thin films for ultra large scale integrated circuits (ULSIs) application—A review." *Journal of Materials Science: Materials in Electronics* 10.1 (1999): 9-31.

⁴⁵ <https://refractiveindex.info/?shelf=main&book=Ta2O5&page=Bright-amorphous>

⁴⁶ Banerjee, Writam, Alireza Kashir, and Stanislav Kamba. "Hafnium oxide (HfO₂)—a multifunctional oxide: a review on the prospect and challenges of hafnium oxide in resistive switching and ferroelectric memories." *Small* 18.23 (2022): 2107575.

⁴⁷ Kol, S., and A. Y. Oral. "Hf-Based High-κ Dielectrics: A Review." *Acta Physica Polonica: A* 136.6 (2019).

⁴⁸ <https://refractiveindex.info/?shelf=main&book=HfO2&page=Al-Kuhaili>

⁴⁹ Abyzov, A. M. "Aluminum oxide and alumina ceramics (review). Part 1. Properties of Al₂O₃ and commercial production of dispersed Al₂O₃." *Refractories and industrial ceramics* 60.1 (2019): 24-32.

⁵⁰ Birey, Hulya. "Dielectric properties of aluminum oxide films." *Journal of applied physics* 49.5 (1978): 2898-2904.

⁵¹ <https://refractiveindex.info/?shelf=main&book=Al2O3&page=Malitson-o>

⁵² Blumenthal, Daniel J., et al. "Silicon nitride in silicon photonics." *Proceedings of the IEEE* 106.12 (2018): 2209-2231.

⁵³ Philipp, Herbert R. "Optical properties of silicon nitride." *Journal of the Electrochemical Society* 120.2 (1973): 295.

⁵⁴ <https://refractiveindex.info/?shelf=main&book=Si3N4&page=Philipp>

⁵⁵ https://en.wikipedia.org/wiki/Fused_quartz

SiO ₂		Fused Silica	Sputter., ALD	available/ L	
Magnesium Fluoride ⁵⁸ , MgF ₂	1.38, 1.39, 1.4 ⁵⁹	Tetragonal	Physical Vapor Deposition (PVD), Sputter.	Excellent transparency, anti-reflection/ Available/L	Used for AR coatings/ Brittle, difficult to deposit thick layers
Lanthanum Fluoride ^{60,61,62} , LaF ₃	1.54, 1.55, 1.56 ⁶³	Hexagonal	PVD, EBD, PLD	Ideal for anti-reflective coatings / Available/M	Excellent transparency and low absorption, low n , High chemical and thermal stability / Requires precise deposition control; Moisture Sensitive, need encapsulation
Lithium Fluoride ^{64,65} , LiF	1.386, 1.389, 1.392 ⁶⁶	Cubic	Thermal evaporation, electron-beam evaporation, sputter.	Ideal for anti-reflective coatings / Available/M	Extremely low refractive index; excellent transparency in both UV and visible regions/ Moisture Sensitive, requiring careful encapsulation
Calcium Fluoride ^{67,68} , CaF ₂	1.429, 1.432, 1.435 ⁶⁹	Crystalline (Cubic)	Thermal evaporation, electron-beam evaporation, sputter.	Ideal for visible and UV optics/ Available/M	Excellent transmission, low dispersion, good chemical stability / Soft and fragile, minor moisture sensitivity

It is worth stressing that, at visible frequency, the available choices for high-refractive index materials are rather limited. Considering also the corresponding manufacturing methods, their quality, and compatibility with existing processes (e.g. lithography after thin film depositions, C-MOS compatibility) this limited choices and combinations have profound implications in terms of best performances and devices costs.

For the low refractive index materials side, beyond SiO₂, that is broadly available, fluorine compounds supply can be complicated by issues primarily concerning raw material sourcing, manufacturing processes, environmental impact, and handling safety.

3. THIN FILM DEPOSITION METHODS

Thin film deposition methods are techniques used to deposit layers of materials with controlled thickness onto a substrate. They fall into three main categories: **physical-, chemical-, and solution-based-deposition methods**^{70, 71, 72}:

Physical deposition includes Physical Vapour Deposition (PVD) techniques such as **sputtering, evaporation, and Pulsed Laser Deposition (PLD)**, where material is physically transferred from a target to the substrate. **Ion Beam Deposition (IBD)** and **Electron Beam Deposition (EBD)** also fall into this category. Each method offers trade-offs in terms of **film quality, uniformity, deposition rate, temperature requirements, deposition speed and costs**, making them suitable for different applications in **optics, electronics, and nano-technology**.

⁵⁶ Leviton, Douglas B., and Bradley J. Frey. "Temperature-dependent absolute refractive index measurements of synthetic fused silica." *Optomechanical Technologies for Astronomy*. Vol. 6273. SPIE, 2006.

⁵⁷ <https://refractiveindex.info/?shelf=main&book=SiO2&page=Franta>

⁵⁸ Dodge, Marilyn J. "Refractive properties of magnesium fluoride." *Applied optics* 23.12 (1984): 1980-1985.

⁵⁹ <https://refractiveindex.info/?shelf=main&book=MgF2&page=Li-o>

⁶⁰ Uhlig, H., et al. "Lanthanide tri-fluorides: a survey of the optical, mechanical and structural properties of thin films with emphasis of their use in the DUV-VUV-spectral range." *Advances in Optical Thin Films II*. Vol. 5963. SPIE, 2005.

⁶¹ Fujihara, Shinobu, Munehiro Tada, and Toshio Kimura. "Sol-gel processing of LaF₃ thin films." *Journal of the Ceramic Society of Japan* 106.1229 (1998): 124-126.

⁶² Pesonen, Leevi. "Rare Earth Fluoride Thin Films." (2024).

⁶³ <https://refractiveindex.info/?shelf=main&book=LaF3&page=Laihoa-o>

⁶⁴ Dauer, Véronique. "Optical constants of lithium fluoride thin films in the far ultraviolet." *Journal of the Optical Society of America B* 17.2 (2000): 300-303.

⁶⁵ Baldacchini, Giuseppe. "Colored LiF: an optical material for all seasons." *Journal of luminescence* 100.1-4 (2002): 333-343.

⁶⁶ <https://refractiveindex.info/?shelf=main&book=LiF&page=Li>

⁶⁷ Wen, Chao, and Mario Lanza. "Calcium fluoride as high-k dielectric for 2D electronics." *Applied Physics Reviews* 8.2 (2021).

⁶⁸ Hahn, Daniel. "Calcium fluoride and barium fluoride crystals in optics: multispectral optical materials for a wide spectrum of applications." *Optik & Photonik* 9.4 (2014): 45-48.

⁶⁹ <https://refractiveindex.info/?shelf=main&book=CaF2&page=Li>

⁷⁰ Chaudhari, Mandakini N., Rajendrakumar B. Ahirrao, and Sanabhau D. Bagul. "Thin film deposition methods: A critical review." *Int. J. Res. Appl. Sci. Eng. Technol* 9.6 (2021): 5215-5232.

⁷¹ Budida, Jyothi, and Kamala Srinivasan. "Review of thin film deposition and techniques." *Materials today: proceedings* 92 (2023): 1030-1033.

⁷² Toma, F. T. Z., et al. "Thin film deposition techniques: a comprehensive review." *J Mod Nanotechnol* 4.6 (2024).

Chemical deposition involves chemical reactions to form thin films. It includes Chemical Vapour Deposition (CVD), Atomic Layer Deposition (ALD), and Sol-Gel processing. Variants like Metal-Organic CVD (MOCVD), Liquid Phase CVD (LPCVD), and Plasma-Enhanced CVD (PECVD) allow for better control of film properties.

Solution-based techniques, such as spin coating, dip coating, and spray coating enable low-cost deposition, particularly for sol-gel and polymer-based materials.

Table 2 *Thin Film Deposition Methods* provides a comparative overview of the most common techniques used for thin film fabrication. It details key parameters such as deposition speed, material purity, thickness control (resolution), surface roughness (RMS), typical deposition temperature, and compatible materials. Additionally, it highlights the advantages and limitations of each method. The table serves as a reference for selecting the appropriate deposition technique based on film quality, process scalability, and application requirements.

TABLE 2. Thin Film Deposition Methods						
Method. Main Features	Deposit. Speed	Purity: Medium M, High H	Thickness Control/ Roughness RMS	Deposit Temp.	Materials	Pros/Cons
Solution-Based Methods						
Spin ⁷³ , Dip-Coating ⁷⁴ , Inkjet ⁷⁵ , Spray Pyrolysis ⁷⁶	10-1000 nm/min	M	~10-50 nm/ 1-100 nm	100-600°C	Polymers, Metal-Oxides, Perovskites	Low-cost, large-area, versatile composition, simple, scalable, compatible with flexible substrates/ High-temperature annealing, shrinkage, poor thickness uniformity, defects from drying
Chemical Vapor Deposition (CVD) Methods						
CVD. Gas-phase reaction of precursors on a heated surface ⁷⁷	10-1000 nm/min	H	~10 nm/ 1-10 nm	300-1200°C	Si, SiO ₂ , Si ₃ N ₄ , Diamond, Metal-Oxides, III-V	High-purity films, good step coverage/High temperature, toxic precursors
MOCVD. Uses metal-organic precursors for compound semiconductors ⁷⁸	50-500 nm/min	H	~1-5 nm/ <1 nm	500-1200°C	III-V semicon.	High-quality films, controlled doping/Complex chemistry, expensive
LPCVD. CVD at reduced pressure for better uniformity ⁷⁹	10-200 nm/min	HH	~1-2 nm/ <1 nm	500-1000°C	Si, Al ₂ O ₃ , Si ₃ N ₄ , SiO ₂ (phospho- and boro-silicate)	Excellent thickness control, uniform/High temperature, slow process
Atomic Layer Deposition, ALD. Layer-by-layer growth via self-limiting reactions ⁸⁰	0.1-2 nm/min	HH	<0.1 nm <1 nm	50-400°C	Metal-Oxides, Nitrides, Sulfides	Atomic precision, excellent step coverage/Slow, expensive precursors
Physical Vapor Deposition (PVD) Methods						
Sputtering (magnetron). Uses plasma to eject material from a target ⁸¹	10-300 nm/min	H	~1-5 nm/ 1-5 nm	20-600°C	Metals, Oxides, Nitrides, Semicon.	High purity, good adhesion/Requires vacuum, high energy
Electron Beam Deposition (EBD). Uses an electron beam to evaporate material ⁸²	10-200 nm/min	H	~1-2 nm/ 1-5 nm	100-600°C	Metals, Oxides, Dielectrics	High-purity films, good control/Some materials decompose under e-beam
Ion Beam Deposition (IBD). Uses ion bombardment for dense, high-purity films ⁸³	1-10 nm/min	HH	~1-10 nm/ 0.5-2 nm	20-400°C	Dielectrics, Metal-Oxides, Metals	High-quality, dense films, precise control/Slow, expensive equipment

⁷³ Mustafa, Haveen Ahmed Mustafa, and Dler Adil Jameel. "Modeling and the main stages of spin coating process: A review." *Journal of Applied Science and Technology Trends* 2.02 (2021): 119-123.

⁷⁴ Brinker, C. Jeffrey. "Dip coating." *Chemical solution deposition of functional oxide thin films*. Vienna: Springer Vienna, 2013. 233-261.

⁷⁵ Shah, Muhammad Ali, et al. "Classifications and applications of inkjet printing technology: a review." *Ieee Access* 9 (2021): 140079-140102.

⁷⁶ Perednis, Dainius, and Ludwig J. Gauckler. "Thin film deposition using spray pyrolysis." *Journal of electroceramics* 14.2 (2005): 103-111.

⁷⁷ Sun, Luzhao, et al. "Chemical vapour deposition." *Nature Reviews Methods Primers* 1.1 (2021): 5.

⁷⁸ Williams, John O. "Metal organic chemical vapor deposition (MOCVD) perspectives and prospects." *Angewandte Chemie International Edition in English* 28.8 (1989): 1110-1120.

⁷⁹ Kern, W., and George L. Schnable. "Low-pressure chemical vapor deposition for very large-scale integration processing—a review." *IEEE Transactions on Electron Devices* 26.4 (2005): 647-657.

⁸⁰ Johnson, Richard W., Adam Hultqvist, and Stacey F. Bent. "A brief review of atomic layer deposition: from fundamentals to applications." *Materials today* 17.5 (2014): 236-246.

⁸¹ Kelly, Peter J., and R. Derek Arnell. "Magnetron sputtering: a review of recent developments and applications." *Vacuum* 56.3 (2000): 159-172.

⁸² Wang, Zhongping, and Zengming Zhang. "Electron beam evaporation deposition." *Advanced nano deposition methods* (2016): 33-58.

Pulsed Laser Deposition (PLD). Uses high-power laser pulses to vaporize material ^{84 85}	1-10 nm/min	HH	~1 nm/ 1-5 nm	100-900°C	Oxides, Nitrides, Supercon.	Good stoichiometry, suitable for complex materials/ Expensive, rougher films
Thermal Evaporation. Heats material in vacuum to evaporate it ⁷¹	10-100 nm/min	HH	~5-10 nm/ 1-10 nm	100-600°C	Metals, Organic Semicon.	Simple, high deposition rate/ Poor step coverage, thickness variation
MBE. Ultra-high vacuum technique using atomic beams for epitaxial growth	~0.01-1 nm/min	HHH	<0/1 nm/ <0.5 nm	300-1000°C	III-V and IV-IV, Oxides	Highest purity and precision, atomic-layer control/ Extremely slow, expensive

4. SOLNIL'S WAY: INORGANIC RESIST SOLUTIONS FOR OPTICAL THIN FILMS MADE OF FULLY INORGANIC MATERIALS

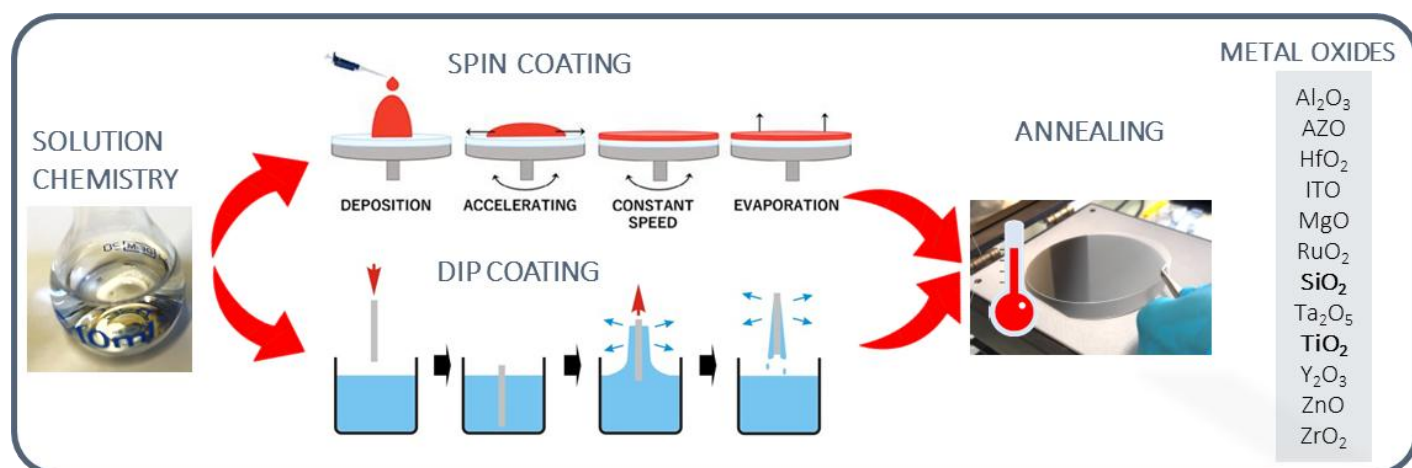


Fig.4. From the left to the right are shown the main technological bricks for the fabrication of metal-oxide-based thin films, including: solution chemistry, spin- (Figure from [K. Waszkowska PhD](#)) or dip-coating (Figure from [coating.de](#)) followed by annealing. SOLNIL's focus is on TiO_2 and SiO_2 as paradigms of high and low refractive index materials.

The previous discussion has detailed the spectrum of thin film deposition methods-ranging from physical, chemical and liquid deposition techniques-and their respective advantages and limitations in achieving high-quality optical coatings. These conventional methods typically offer exceptional control over film uniformity and purity. However, they often require complex, high-temperature, or high-vacuum conditions that can drive up costs and limit scalability.

Here, we introduce SOLNIL's approach based on liquid chemistry and deposition^{86 87 88} (Fig.4). These methods leverage simple, ambient-pressure processes such as spin- and dip-coating to deposit fully inorganic thin films, offering a cost-effective and scalable alternative with the added benefit of tuneable optical properties. By precisely controlling factors like porosity and crystallinity, SOLNIL's solutions bridge the gap between performance and manufacturability, paving the way for next-generation optical coatings in photonic devices. SOLNIL's materials and related deposition methods encompass the common limitations of liquid deposition processes enabling record performances in this category and beyond, as accounted for the deep characterization of the final product in terms of optical quality, thermal and chemical stability, and mechanical strength (Table 3 *SOLNIL's ultra-low and ultra-high refractive index materials*).

SOLNIL delivers a broad variety of metal oxides (MOx, such as TiO_2 and SiO_2) materials for applications in optics and photonics at visible frequency. The underlying chemistry is a versatile wet-chemical method used for synthesizing metal oxide materials through the formation of a colloidal sol, which then transitions into a gel network. This process typically involves hydrolysis and condensation reactions of metal alkoxides or inorganic salts in solution:

⁸³ Mohan, S., and M. Ghanashyam Krishna. "A review of ion beam assisted deposition of optical thin films." *Vacuum* 46.7 (1995): 645-659.

⁸⁴ Soonmin, Ho. "A brief review of the growth of pulsed laser deposited thin films." *British Journal of Applied Science & Technology* 14.6 (2016): 1.

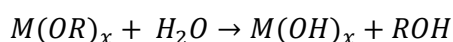
⁸⁵ Cheung, Jeffrey T., and Haluk Sankur. "Growth of thin films by laser-induced evaporation." *Critical Reviews in Solid State and Material Sciences* 15.1 (1988): 63-109.

⁸⁶ Danks, Ashleigh E., Simon R. Hall, and Z. J. M. H. Schnepf. "The evolution of 'sol-gel' chemistry as a technique for materials synthesis." *Materials Horizons* 3.2 (2016): 91-112.

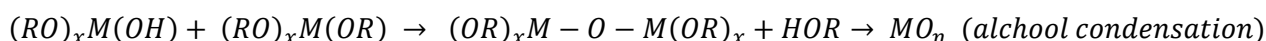
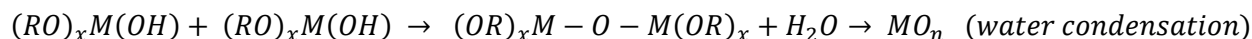
⁸⁷ Hench, Larry L., and Jon K. West. "The sol-gel process." *Chemical reviews* 90.1 (1990): 33-72.


⁸⁸ de Souza, Arthur Clini, et al. "Méthodes de dépôt liquide de matériaux inorganiques pour la photonique." *Photoniques* 133 (2025): 19-21.

- **Hydrolysis:** Metal alkoxides ($M(OR)_x$) react with water, leading to the replacement of alkoxide groups ($-OR$) with hydroxyl groups ($-OH$), forming metal-hydroxo species:



- **Condensation:** The hydroxyl groups undergo condensation, linking metal centres through $M - O - M$ bonds, leading to the formation of a growing network that evolves into a gel:



		
Table 3. SOLNIL's ultra-low and ultra-high refractive index materials		
FEATURE	SILICA SiO_2	TITANIA TiO_2
Max thickness deposited in one single step	2600 nm \pm 3% (larger values achieved by multi-layer deposition)	100 nm \pm 3% (1000 nm achieved by multi-layer deposition)
Surface roughness (RMS, nm)	1 nm for $n = 1.12$ 0.4 for $n = 1.38$	<0.5 nm up to $n = 2.6$
n@520nm	1.08-1.45 \pm 0.005	1.70-2.60 \pm 0.01
Haze	<0.05%	<0.2% for $n < 2.5$ <0.5% for $2.5 < n < 2.6$
Abs. (scattering losses)	<0.05% RGB	<0.2% RGB
Curing temperature	300-450 °C	100-800 °C
Young Modulus	\approx 2 GPa	\approx 200 GPa
Relative Humidity RH 85% at 85°C x 72 h	$\Delta n = 0.01$	
UV light 1h, 306 W/cm ² @ 365 nm	$\Delta n \approx 0$	
Thermal shock, -30°C to + 60°C x 100 cycles	$\Delta n \approx 0$	
Processability	Spin-coating, Dip-coating, Nano-Imprint	
Solution shelves life	>2 months at 6 °C	
Laser dicing	No delamination	

The relative kinetics of hydrolysis and condensation governs the formation of the final materials into polymeric fractal gels or densified objects (oxoclusters, nano-particles) dispersions in solution. At this stage, the solution is processed as thin film, and a final thermal curing is applied to form the final materials. Crystallinity, density are controlled by the thermal budget. Starting from liquid solutions, this approach allows depositing thin films with very simple and versatile methods such as spin- and dip-coating, as well as spraying coating. Upon annealing and evaporation of the volatile compounds, this method allows precise control over composition, porosity, and structure, making it ideal for applications in **optics, coatings, catalysis, and electronics**.

Unlike conventional deposition methods, that use expensive machines, controlled atmosphere (e.g. ultra-high vacuum), and dangerous gasses, SOLNIL's approach works at room temperature and atmospheric pressure, rendering the deposition process extremely cheap and fast. After deposition via spin- or dip-coating, the process is finalised by high-temperature annealing (100-800 °C, depending on the substrate tolerances, final refractive index, desired porosity, etc.) for times ranging from few minutes to

hours in a simple induction oven.

4.1. SOLNIL'S ULTRA-HIGH AND ULTRA-LOW REFRACTIVE INDEX MATERIALS

Here we focus on two of the most important cases for optics and photonics at visible frequency: silica⁸⁹ (SiO_2) and titania⁹⁰ (TiO_2). They can be both produced over large wafers with high planarity and low roughness, limiting scattering losses (Table 3, and Fig.5-7).

SOLNIL's silica (SiO_2) can be processed as thin film by spin or dip deposition with a thickness exceeding 2600 nm in a single passage. Thicker layers can be produced by subsequent deposition steps. Annealing from 300 to 450 °C creates a highly homogeneous, robust and water resistant, fully inorganic (polymer-free) SiO_2 network with refractive index ranging from 1.12 (ULRI, Fig.5) to 1.45 \pm 0.005 RIU. Precise adjustment of the refractive index is achieved by adding porosity to the thin film. It can be deposited at room temperature and atmospheric pressure as well as printed in 3D structures by thermal soft nano-imprint lithography. This ultra-low refractive index silica can be used for encapsulation of meta-surfaces or as cladding layer of photonic integrated circuits.

⁸⁹ Grosso, D., et al. "Two-dimensional hexagonal mesoporous silica thin films prepared from block copolymers: Detailed characterization and formation mechanism." *Chemistry of Materials* 13.5 (2001): 1848-1856.

⁹⁰ O'Byrne, Martin, et al. "Investigation of the anatase-to-rutile transition for TiO_2 sol-gel coatings with refractive index up to 2.7." *Thin Solid Films* 790 (2024): 140193.

14

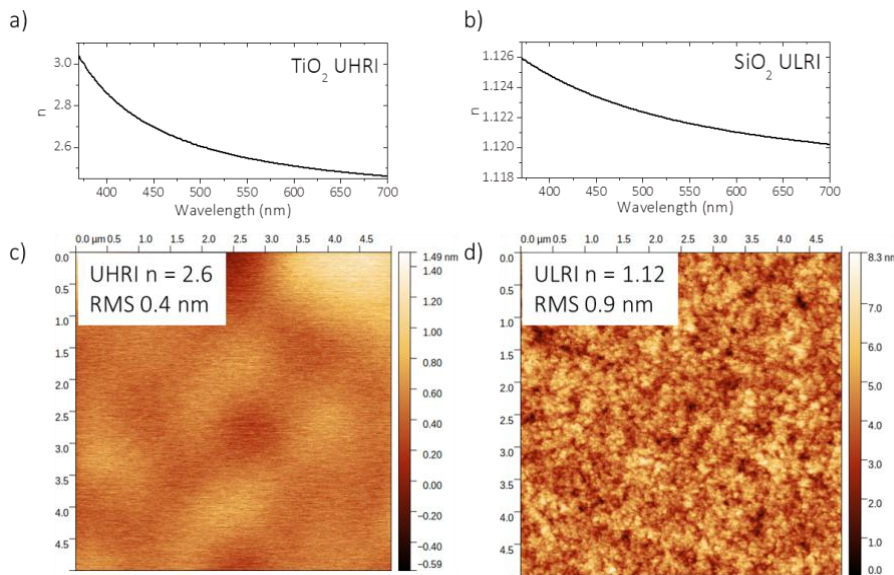


Fig.5. a) and b) Ellipsometric measurement of the refractive index of UHRI TiO_2 and ULRI SiO_2 , respectively. c) Absorption losses for TiO_2 with refractive index RI up to 2.6 (UHRI). d) Atomic force microscope (AFM) image of the UHRI surface. e) Atomic force microscope (AFM) image of the ULRI surface.

prepared by successive depositions). After curing, high density homogeneous titania coatings are obtained, exhibiting **refractive index n up to 2.60 ± 0.01 (at 520 nm, UHRI, Fig.5)**. Precise adjustment of the refractive index is achieved by playing with the crystalline state of the thin film (e.g. from amorphous to pure anatase, Fig.6-7). **These coatings showcase very low haze and absorption (Table 3), even for high index materials, thanks to the sub-20 nm anatase grains compacted into a dense (non-porous) composite (Fig.6-7)**. The material can be printed by thermal soft-nano imprint lithography in 3D patterns.

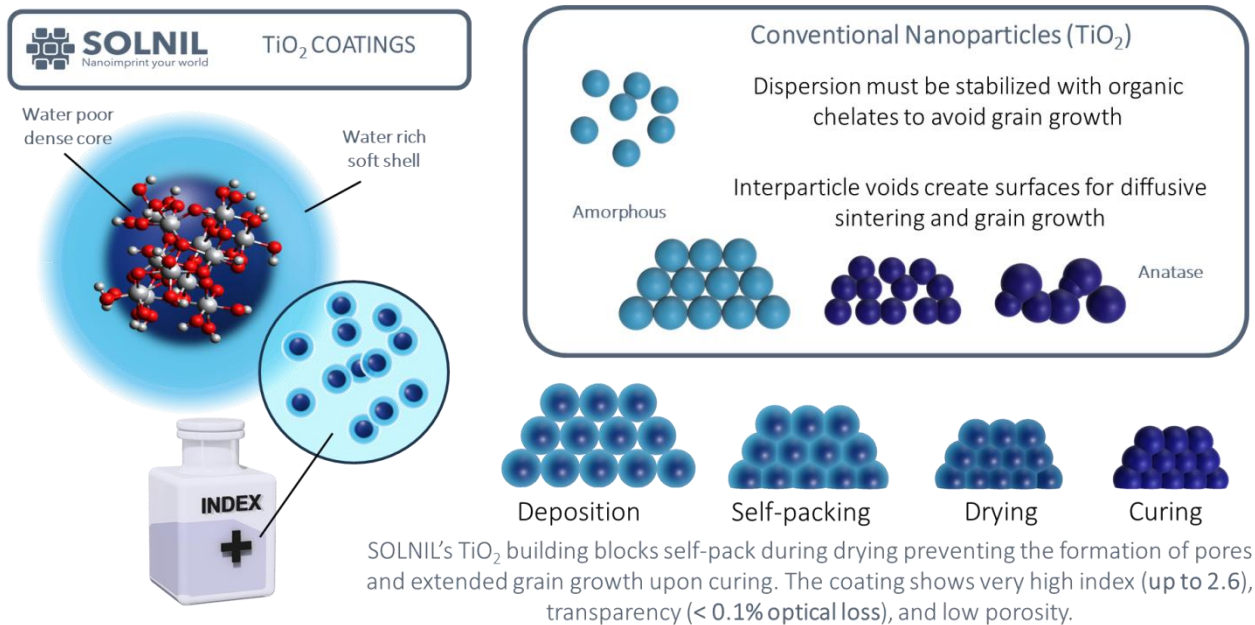


Fig.6. Left and bottom: SOLNIL process of TiO_2 self-packing for refractive index RI up to 2.6 (UHRI). Top right: conventional TiO_2 particles self-packing resulting in porosity and grain growth, lowering the refractive index and increasing scattering.

Liquid chemistry offers several notable advantages for depositing TiO_2 :

- its simplicity and cost-effectiveness;
- it **does not require expensive high-vacuum equipment** and can be performed under ambient conditions, making it accessible for large-area processing;
- liquid chemistry methods provide high throughput and are well suited for coating complex shapes, thanks to the solution-based nature of the process;

Unlike other examples of highly porous materials (e.g. aerogels, 'frozen smoke'), **SOLNIL provides a highly stable SiO_2 from thermal, chemical, and mechanical standpoints**. Very importantly:

- SOLNIL ULRI SiO_2 is highly transparent across the visible spectrum with scattering losses below 0.05%
- it is of optical quality with an overall RMS < 1 nm
- it can be deposited with extremely low thickness fluctuations across 6 inches wafers ($\pm 3\%$)
- it is hydrophobic (n changes about 0.01 RIU upon 80% humidity increase).

SOLNIL's titania (TiO_2 , Fig.5-7) can be processed as thin film with thickness up to 100 nm in a single passage by spin or dip deposition (larger thickness can be

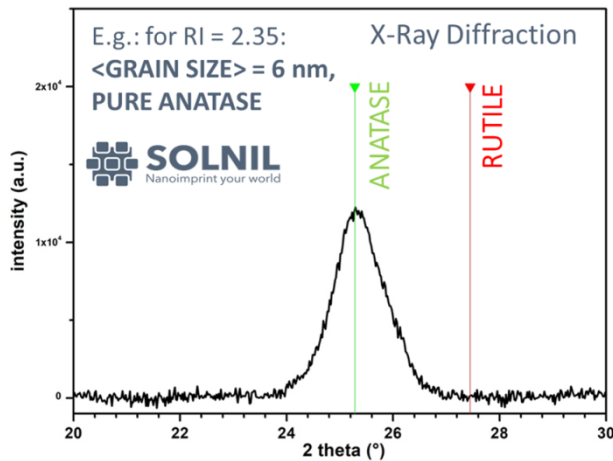


Fig.7. X-Ray diffraction spectroscopy of SOLNIL's TiO_2 with refractive index $n = 2.35$. This analysis points out the composition of the material as pure anatase (the rutile phase is completely absent) and the grain size, that is in the range of 6 nm. Generally speaking, for $n = 2.57$ we find a grain size below 20 nm in average⁹⁰.

-it allows for easy incorporation of dopants and additives to tailor the film properties⁹¹, as well as **flexibility in tuning the microstructure through controlled drying and annealing**.

While ALD excels in precise thickness control and conformality at the nano-scale, SOLNIL's liquid chemistry is an attractive alternative when ultra-precise layer control is less critical and cost or scalability is a primary concern.

Conventional sol-gel chemistry is highly sensitive to processing conditions such as humidity, pH, and drying rate. This sensitivity can lead to issues like uncontrolled porosity and cracking, primarily due to significant shrinkage during solvent evaporation and calcination⁹². Moreover, achieving uniform film thickness and excellent crystallinity (or a specific phase, such as anatase) is challenging. Residual organic impurities and difficulties in precisely controlling the stoichiometry further affect the optical properties of the films.

SOLNIL went beyond these issues. Unlike other examples of metal oxides obtained from liquid solutions that leave a

porous matrix after annealing (e.g. requiring for further processing to increase the refractive index), SOLNIL high- n TiO_2 is delivered with a full control over crystalline state and porosity. In particular:

- SOLNIL's original inorganic resin formulation undergoes a self-packing of core-shell nano-particles
- the porosity of the final material is reduced to minimal values (< 3-4%) allowing for ultra-high refractive index
- pure anatase poly-crystal with average size below 20 nm keep the scattering losses low across the visible spectrum
- surface roughness is limited to <0.5 nm, providing high quality interfaces and reducing light scattering.

4.2. SOLNIL: TWO SOLUTIONS FOR ALL THE REFRACTIVE INDICES

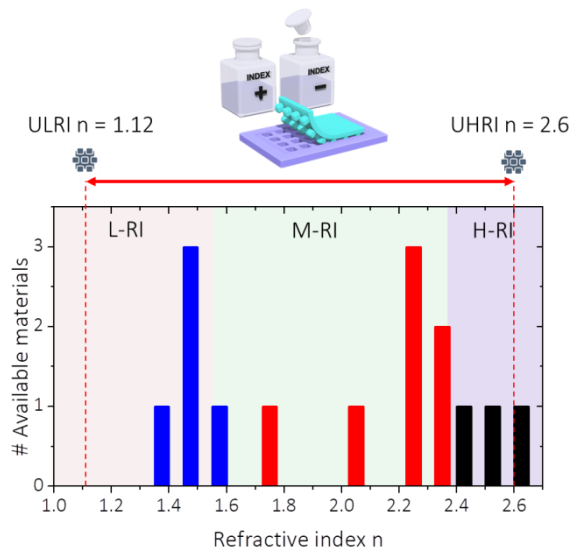


Fig.8. Statistical distribution of refractive index n for the materials usable at visible frequency (from Table 1). The refractive index (RI) is split into three intervals: low, medium and high, respectively L-RI ($n < 1.5$), M-RI ($1.5 < n < 2.3$), and H-RI ($2.3 < n < 2.6$). The vertical dashed lines highlight the values of n for SOLNIL's ULRI and UHRI. The two solutions for TiO_2 and SiO_2 are miscible in any proportion and all the values of n between ULRI and UHRI can be obtained.

The refractive index of inorganic, intrinsic, stoichiometric, and dense materials comes with well-defined values. Within the low-, medium and high-refractive index (respectively L-RI, M-RI, and H-RI, Fig.8), lay several gaps, not covered by any compound transparent at visible frequency: for instance, the ranges $n = 1.55$ -1.70 and 1.70-2.0. At the same time, for very low values, below 1.38, there are no inorganic materials available. There are thus several viable solutions to adjust the refractive index to specific needs.

Compositional engineering (Fig.9), such as altering the stoichiometry of materials⁹³, demands extremely tight control over the chemical composition. Small deviations can lead to phase separation or non-uniformity in the optical properties, and the material's thermal and mechanical stability may also be compromised. In nano-composites, where high-index nano-particles (e.g., TiO_2 or ZrO_2) are dispersed within a lower-index matrix, a key issue is ensuring that the nano-particles remain uniformly dispersed. **Any agglomeration can cause unwanted light scattering and absorption losses**, thus reducing the overall

transparency and degrading the desired optical performance.

⁹¹ Chehadi, Zeinab, et al. "Soft Nano-Imprint Lithography of Rare-Earth-Doped Light-Emitting Photonic Metasurface." *Advanced Optical Materials* 10.21 (2022): 2201618.

⁹² Bottein, Thomas, et al. "Environment-controlled sol-gel soft-NIL processing for optimized titania, alumina, silica and yttria-zirconia imprinting at sub-micron dimensions." *Nanoscale* 10.3 (2018): 1420-1431.

⁹³ Perkins, Joshua, et al. "Color tunable, lithography-free refractory metal-oxide metacoatings with a graded refractive index profile." *Nano Letters* 23.7 (2023): 2601-2606.

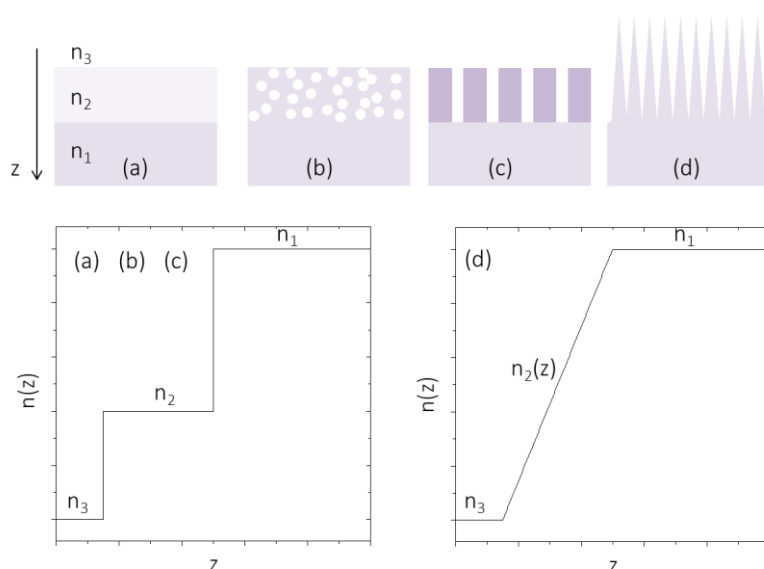


Fig.9. a) Substrate with refractive index n_1 topped with a thin film with refractive index n_2 , surrounded by a medium of refractive index n_3 . b) The substrate material is topped with a porous matrix lowering the refractive index of the top layer. c) The substrate is topped with a nano-structure array resulting in an effective medium with lower refractive index. d) The substrate material is nano-structures with conical structures creating an effective medium with variable refractive index. a), b) and c) cases can be all represented as a thin film atop the substrate (bottom left). The case d) represents the adiabatic index matching configuration, where the passage from the environment with refractive index n_3 to the substrate with refractive index n_1 occurs smoothly substrate (bottom right).

Hybrid organic-inorganic materials prepared via sol-gel processes allow for tuning the refractive index by incorporating various precursors or additives⁹⁴. However, these materials may suffer from processing challenges such as incomplete network formation, phase separation, or aging effects (like yellowing under UV light) in case organic compounds are used, all of which can alter the optical clarity and long-term stability of a device. Atomic layer deposition offers precise control over film thickness and composition, but suffers from an inherently slow deposition rate and its high cost can limit its scalability for large-area or high-throughput applications.

For materials with refractive indices below ~ 1.38 , it is possible to “dilute” the optical density⁹⁵ (Fig.9 b)). One common approach is to introduce controlled porosity into an otherwise dense material, effectively mixing the material with air ($n \approx 1.0$) so that the overall, effective refractive index is reduced⁹⁶. Another strategy is to use inherently low-index organic materials, often fluorinated polymers⁹⁷, which naturally exhibit refractive indices in this lower range. A third method is to engineer

nano-composites by embedding low-index fillers into a host matrix, thereby adjusting the effective refractive index according to effective medium theories.

Another powerful approach is nano-structuring⁹⁵ (Fig.9 c) and d)). By engineering the material on a sub-wavelength scale (for example, creating periodic nano-patterns), exploiting effective medium theories it is possible to obtain a “designer” refractive index. These strategies are particularly relevant because they enable the fabrication of components like anti-reflective coatings, waveguides, and meta-materials with precisely controlled optical properties.

Each of these approaches comes with potential issues. In porous materials, the creation of voids can compromise mechanical strength and environmental durability; additionally, the presence of pores may introduce unwanted light scattering or diffraction losses if the pore size and distribution are not carefully controlled. Low-index fluoropolymers, while promising for their naturally low refractive indices, can be challenging to process and may exhibit sensitivity to environmental factors such as moisture or UV exposure. Finally, in nano-composites the key challenge lies in achieving a uniform dispersion of the low-index phase, whether that’s air, nano-particles, or another filler, without agglomeration or phase separation, which would otherwise lead to non-uniform optical properties and additional scattering losses. Thus, while these methods offer practical pathways to reach refractive indices below 1.38, they require tight control over the fabrication processes to balance optical performance, mechanical stability, and long-term durability.

SOLNIL’s chemistry allows a perfect mixing of the inorganic resins used for ultra-low and ultra-high refractive index materials (Fig.8). As such, the refractive index gap between dense SiO_2 and amorphous TiO_2 ($n = 1.45\text{--}2$) can be covered: thanks to the perfect miscibility of the two solutions in any proportion, a wide and fine adjustment of the optical constant is possible from 1.12 up to 2.60 by introducing controlled porosity for low indices and by tuning the crystallinity for high indices (larger values of n are also possible; however, entering in the rutile phase of TiO_2 adds unwanted scattering losses at short wavelength and are not considered here).

⁹⁴ Parola, Stephane, et al. "Optical properties of hybrid organic-inorganic materials and their applications." *Advanced Functional Materials* 26.36 (2016): 6506-6544.

⁹⁵ Modaresialam, Mehrnaz, et al. "Nano-imprint lithography of broad-band and wide-angle antireflective structures for high-power lasers." *Optics Express* 32.7 (2024): 12967-12981.

⁹⁶ Vincent, Abhilash, et al. "Role of catalyst on refractive index tunability of porous silica antireflective coatings by sol-gel technique." *The Journal of Physical Chemistry C* 111.23 (2007): 8291-8298.

⁹⁷ Guerre, Marc, et al. "Solution self-assembly of fluorinated polymers, an overview." *Polymer Chemistry* 12.27 (2021): 3852-3877.

4.3. IMPACT OF THE REFRACTIVE INDEX CONTRAST

Snell's law is a fundamental principle in optics that describes how light changes direction, i.e. refracts-when it passes from one medium into another. It is given by: $n_1 \sin \theta_1 = n_2 \sin \theta_2$, where n_1 and n_2 are the refractive indices of the first and second media, and θ_1 and θ_2 are the angles the light ray makes with the normal in each medium⁸ (an imaginary line perpendicular to the surface, Fig.10). When light moves from a less optically dense medium (lower n) into a denser medium (higher n), it slows down and bends toward the normal. Conversely, if light travels from a denser to a less dense medium, it speeds up and bends away from the normal. However, there's a special situation when light attempts to pass from a denser medium into a rarer one: if the angle of incidence exceeds a certain threshold, known as the critical angle θ_c , the refracted ray no longer exists. Instead, all the light is reflected back into the denser medium, a phenomenon called **total internal reflection (Fig.10)**. The critical angle θ_c can be found by setting the angle of refraction to 90 degrees in Snell's law: $\theta_c = \arcsin(n_2/n_1)$, where n_1 is the refractive index of the denser medium and n_2 that of the rarer medium. **The largest is the refractive index contrast (that is, the smaller is the ratio n_2/n_1), the smaller is θ_c implying that rays propagating closer to normal incidence stay confined in the high-refractive index medium.**

This principle underpins many technologies, such as guided optics, where light is confined within a medium by repeated total internal reflections^{98, 99}: in practice, increasing the refractive index contrast allows to fit smaller propagating angles (with respect to normal incidence) for light. **This has many consequences, as, for instance, increasing the field of view of for virtual images in augmented reality devices based on waveguides. As such, having materials with ultra-high and ultra-low refractive index is crucial for providing a fully immersive augmented reality experience.**

4.3.1. LIGHT GUIDING

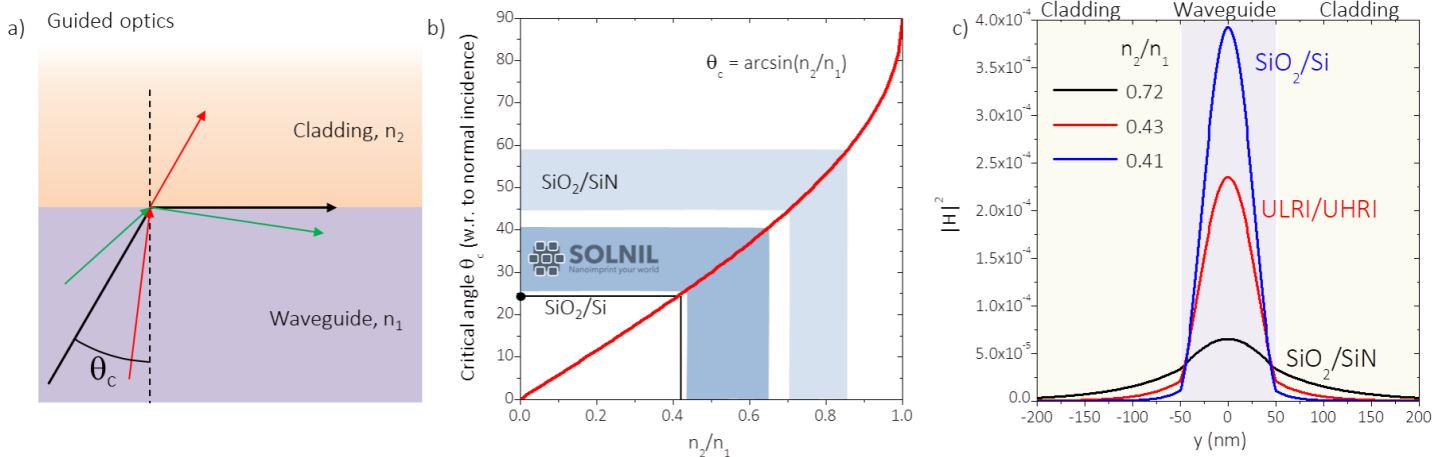


Fig.10. a) Snell's law representation and critical angle θ_c for total internal reflection: light propagating at angles smaller than θ_c are partially transmitted, whereas those propagating at larger angles stay confined in the high refractive index medium (green ray). b) Critical angle θ_c as a function of the refractive index contrast n_2/n_1 between cladding and waveguide. c) Mode confinement in a planar waveguide for three relevant cases representative of the SiO₂/Si, SiO₂/SiN and the ULRI/UHRI systems. Note that only the ULRI/UHRI and SiN/SiO₂ cases are relevant to visible frequency light.

A relevant application of photonic devices are waveguides and photonic integrated circuits (PICs, Fig.10): in a waveguide, the ability to confine and guide light efficiently depends on the difference in refractive index between the **core** (high-index) and the **cladding** (low-index). This contrast determines several relevant features: **Mode Confinement** (a smaller n_2/n_1 leads to stronger confinement of light within the waveguide, reducing **radiation losses** and allowing for more compact photonic components), **bending Losses** (smaller n_2/n_1 enables **tighter waveguide bends** without excessive light leakage, which is essential for high-density integration in PICs), **propagation Losses** (low-contrast waveguides with larger n_2/n_1 exhibit more leakage into the cladding, increasing propagation losses, whereas high-contrast waveguides enable efficient light transport), **mode Effective Index and Dispersion** (a smaller n_2/n_1 results in a

⁹⁸ Taylor, Henry F., and Amnon Yariv. "Guided wave optics." *Proceedings of the IEEE* 62.8 (2005): 1044-1060.

⁹⁹ Saleh, Bahaa EA, and Malvin Carl Teich. "Guided-wave optics." *Fundamentals of photonics* 1 (2001).

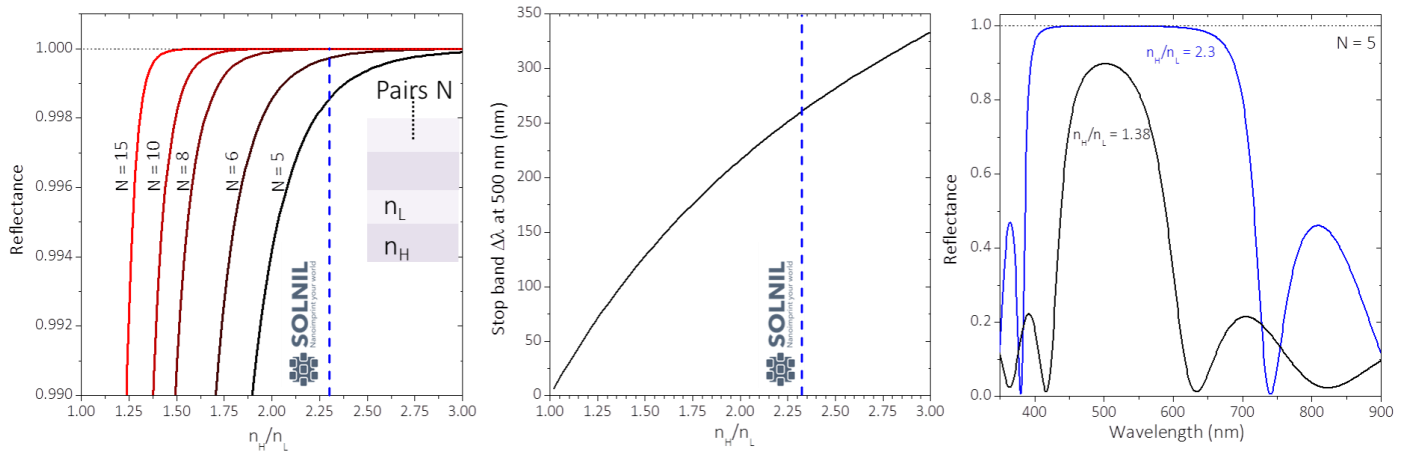
larger difference between the effective index of guided modes and the cladding, impacting **chromatic dispersion**, which is critical for **dispersion engineering** in high-speed optical communication).

For **silicon photonics** (relevant only for near-infrared frequency) the n_2/n_1 provided by Si ($n \approx 3.5$) and SiO₂ cladding ($n \approx 1.45$) reaches the value of about 0.4 that translates into a critical angle θ_c of 23.6 degrees: this allows for **ultra-compact, low-loss waveguides**, making it the dominant platform for modern photonic circuits. However, at visible frequency, Si absorption prevents its use. As such, SiN and SiO₂ are the most common solutions for guiding and cladding materials respectively, for PICs also due to their C-MOS process compatibility. Considering typical values of refractive index for SiN and SiO₂, we obtain a ratio of n_2/n_1 of about 0.72 and a critical angle θ_c limited to about 46 degrees.

Considering SOLNIL's ultra-high (UHRI, $n = 2.6$) and ultra-low (ULRI, $n = 1.12$) refractive index materials, it is possible to get performances very close to those of Si and SiO₂ with the advantage of full transparency also at visible frequency with n_2/n_1 of about 0.43 corresponding to a θ_c of 25.3 degrees, about half of the SiN/SiO₂ system.

4.3.2. BRAGG STRUCTURES

Fig.11. Left panel: Reflectance from a Bragg mirror as a function of the refractive index contrast n_H/n_L of the high- and low-refractive index materials composing the bilayer unity. The curves represent $N = 5$ to 15 pairs of bi-layers. The vertical dashed line highlights the condition obtainable with SOLNIL's ULRI and UHRI materials. Central panel: stop-band $\Delta\lambda$ of a Bragg mirror as a function of n_H/n_L for $\lambda = 532$ nm. The vertical dashed line highlights the condition obtainable with SOLNIL's ULRI and UHRI materials. Right panel: Reflectance spectrum as a function of wavelength for $N = 5$ pairs for ULRI/UHRI ($n_H/n_L = 2.3$) and SiN/SiO₂ cases ($n_H/n_L = 1.38$).



Another important case of photonic structure is the **Bragg mirror** (Fig.11). In this device mirror the refractive index contrast between the two materials used to form a bi-layer plays a central role in determining the mirror's performance^{100, 101, 102}. When light encounters the boundary between a high-index layer and a low-index layer, a portion of it is reflected. A larger refractive index contrast means that a greater fraction of the incident light is reflected at each interface. This increased reflection per interface allows the reflections from successive layers to interfere constructively more effectively at the design wavelength, thereby enhancing the overall reflectivity R of the mirror and the width $\Delta\lambda$ of the stop band¹⁰³ (the range of wavelengths over which the mirror reflects light efficiently).

$$R = \left| \frac{\frac{n_0}{n_S} \left(\frac{n_H}{n_L} \right)^{2N} - 1}{\frac{n_0}{n_S} \left(\frac{n_H}{n_L} \right)^{2N} + 1} \right|^2 \quad \Delta\lambda = \lambda \frac{4}{\pi} \arcsin \left(\frac{\frac{n_H}{n_L} - 1}{\frac{n_H}{n_L} + 1} \right)$$

where n_0 and n_S are the refractive index of the top medium (where the light beam is coming from) and of the substrate, respectively (here we consider air and glass, respectively), n_H and n_L are the refractive indices of the high-

¹⁰⁰ https://en.wikipedia.org/wiki/Dielectric_mirror

¹⁰¹ https://www.rp-photonics.com/dielectric_mirrors.html

¹⁰² Chong, C. K., et al. "Bragg reflectors." *IEEE Transactions on Plasma Science* 20.3 (2002): 393-402.

¹⁰³ <https://www.scientificlib.com/en/Physics/Optics/DistributedBraggReflector.html>

index and low-index materials, and λ is the central wavelength of the stop band. For a quarter-wave stack (each layer having a thickness $L = \lambda/4n$) illuminated at normal incidence, this means that using a higher contrast n_H/n_L one can achieve a high reflectivity R and a broader stop-band width $\Delta\lambda$ with fewer pairs of layers.

With conventional materials working at visible frequency, a high reflectivity (e.g. above 99%) has been achieved only with a relatively large number N of bilayers stack (e.g. $N \sim 10$ for $n_H/n_L \sim 1.38$, corresponding to the conventional case of SiN/SiO_2). In turn, this range of refractive index contrast results in a small stop-band width, well below 100 nm in FWHM, e.g. not sufficient to cover the visible spectrum. On the contrary, exploiting SOLNIL's materials, such as ultra-large and ultra-low refractive index high (UHRI, $n = 2.6$ and ULRI, $n = 1.12$), with just 5 bilayers the reflectivity can go above 99.8% with a stop-band of about 250 nm covering almost the full visible range (Fig.11).

4.3.3. PHOTONIC META-SURFACES

Within the emerging field of dielectric meta-surfaces¹⁰⁴ working at visible frequency, the refractive index contrast between nano-resonators and the background medium¹⁰⁵ plays a key role in tailoring the phase, amplitude, and polarization of light. In realistic applications, the meta-atoms need to be protected (e.g. owing to their scarce mechanical strength of sub-micrometric sized objects) embedding them in a protective (cladding) layer. The refractive index contrast impacts:

-**resonance strength** (a higher index contrast enhances the optical resonances of individual nano-structures, enabling strong field confinement and efficient light manipulation);

-**phase control** (meta-surfaces rely on abrupt phase shifts introduced by resonators; a high index contrast allows full 2π phase control, which is essential for designing high-efficiency meta-lenses and beam-shaping elements). In this context, using conventional materials with a refractive index contrast of 2.3/1.5 delivers a 2π phase shift with meta-atoms having a height of 1200 nm, whereas using SOLNIL's UHRI and ULRI with a contrast of 2.5/1.12 allows to half that length to 600 nm¹⁰⁶. This has important consequences for nano-fabrication.

-**scattering efficiency** (high-index nano-structures strongly scatter light, increasing

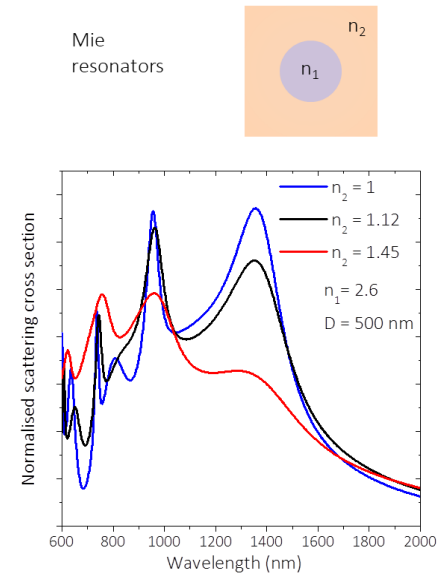


Fig.12. Top: sketch of a spherical Mie resonator with refractive index n_1 embedded in a medium with refractive index n_2 . Bottom: Scattering cross section for a spherical Mie resonator for three refractive index contrast corresponding to $n_1 = 2.6$ (UHRI) and $n_2 = 1$ (air), 1.12 (ULRI), and 1.45 (conventional SiO_2).

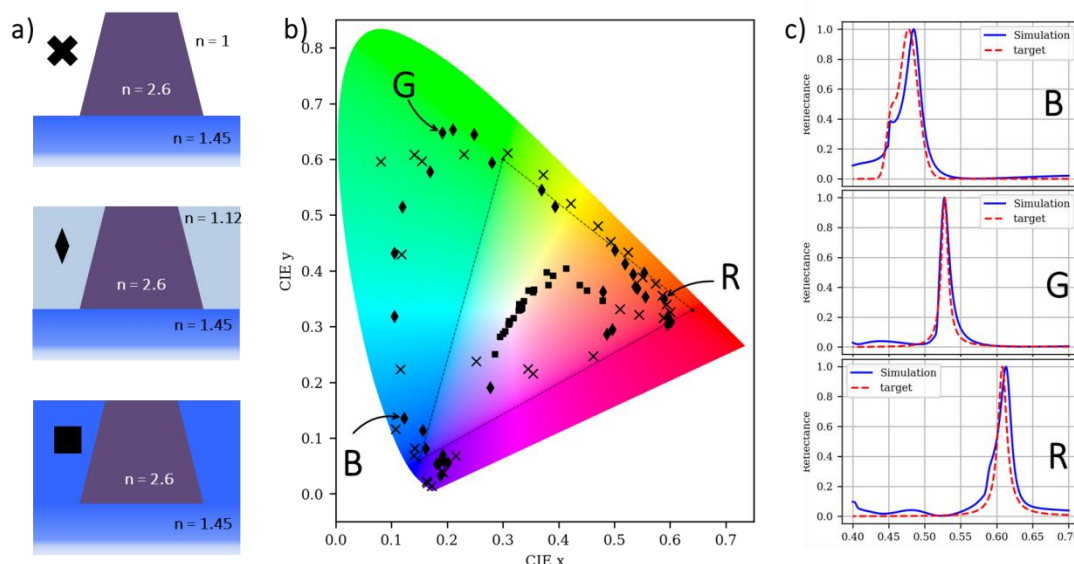


Fig.13. Right: sketches of TiO_2 based ridges (made of high- n TiO_2 UHRI) sitting on glass and embedded in air ($n=1$), ULRI ($n=1.12$), and conventional SiO_2 ($n=1.45$). b) Colour Gamut of the structural colour emerging from infinite arrays of parallel ridges with optimized slanting, height and spacing for the three difference cases shown in a). c) Three selected reflection spectra for R, G and B light.

the efficiency of Huygens' meta-surfaces, dielectric meta-surfaces, and Mie-resonant devices, Fig.13);

-**transmission vs. reflection performance** (low-contrast meta-surfaces, such as polymer-based, tend to operate in gradual phase accumulation modes, whereas high-contrast meta-surfaces, such as TiO_2 or GaN-based, enable sharp phase discontinuities, leading

¹⁰⁴Jahani, Saman, and Zubin Jacob. "All-dielectric metamaterials." Nature nanotechnology 11.1 (2016): 23-36.

¹⁰⁵Van de Groep, J., and A. Polman. "Designing dielectric resonators on substrates: Combining magnetic and electric resonances." Optics express 21.22 (2013): 26285-26302.

¹⁰⁶As deduced using PLANOPSIM software

to better performance in optical beam steering, holography, and wave-front shaping.

A first simple example is a spherical TiO₂-based Mie resonator (with $n = 2.6$, UHRI) surrounded by and the environment having $n = 1$, 1.12 (ULRI) and 1.45, representative of air, porous SiO₂ from SOLNIL and conventional SiO₂, Fig.13). Strong and sharp Mie resonances (electric and magnetic multipolar modes) appear only for high refractive index contrast¹⁰⁵.

A second relevant example for applications of meta-surfaces is structural colour (Fig.13). Avoiding the use of conventional pigments prone to aging, bright and sharp spectra can be created *ad hoc* by nano-structuring a material¹⁰⁷.

The refractive index contrast between the materials in use plays a pivotal role: a higher contrast generally leads to stronger reflections at the interfaces, sharper interference fringes, and hence more vivid, saturated colours with a narrower spectral bandwidth. Conversely, if the refractive index contrast is low, the interference effects become weaker and the resultant colours are often less intense and broader in spectrum.

An example of this is provided by slanted ridges made of SOLNIL's high refractive index TiO₂ (UHRI, $n = 2.6$) on top of conventional glass ($n = 1.45$): when surrounded by air or by ultra-low SiO₂ (ULRI, $n = 1.12$) the corresponding colorimetry showcases saturate colours (e.g. close to the edges of the Gamut), whereas when embedded in conventional SiO₂, the resonances are much broader resulting in colours much closer to white.

5. CONCLUSION

This white paper underscores the transformative potential of inorganic optical coatings in the realm of photonic devices operating at visible frequencies. By exploiting advanced liquid chemistry, SOLNIL has developed innovative, scalable processes for depositing ultra-high and ultra-low refractive index materials with exceptional optical clarity and minimal scattering losses. The ability to precisely control film thickness, porosity, and crystallinity through simple deposition techniques such as spin- and dip-coating at ambient conditions not only offers cost-effective manufacturing but also meets the stringent requirements for next-generation photonic applications. These include high-performance meta-surfaces, photonic integrated circuits, and advanced optical components for emerging technologies in imaging, augmented reality, and quantum photonics. Ultimately, SOLNIL's approach bridges the gap between fundamental material science and practical device fabrication, paving the way for a new era of compact, efficient, and versatile photonic systems.

¹⁰⁷ [Clini de Souza, Arthur, et al. "Back-propagation optimization and multi-valued artificial neural networks for highly vivid structural color filter metasurfaces." *Scientific reports* 13.1 \(2023\): 21352.](#)